

- <sup>15</sup>A. Christy and O. Haüsser, Nucl. Data, (to be published).
- <sup>16</sup>L. G. Multhauf, K. G. Tirsell, and E. A. Nawrocki, Bull. Am. Phys. Soc. **17**, 71 (1962).
- <sup>17</sup>D. Schwalm, A. Bamberger, P. G. Bizzeti, B. Povh, G. A. P. Engelbertink, J. W. Olness, and E. K. Warburton, Nucl. Phys. **A192**, 449 (1972).
- <sup>18</sup>A. E. Litherland and A. J. Ferguson, Can. J. Phys. **39**, 788 (1961).
- <sup>19</sup>A. R. Poletti and E. K. Warburton, Phys. Rev. **137**, B595 (1965).
- <sup>20</sup>A. Z. Schwarzschild and E. K. Warburton, Annu. Rev. Nucl. Sci. **18**, 265 (1972).
- <sup>21</sup>D. B. Fossan and E. K. Warburton, in Nuclear Spectroscopy II, edited by J. Cerny (Academic, New York, to be published).
- <sup>22</sup>D. H. Wilkinson, in *Nuclear Spectroscopy*, edited by F. Ajzenberg-Selove (Academic, New York, 1960).
- <sup>23</sup>J. P. Coffin, A. Gallmann, F. Haas, P. Wagner, and J. W. Olness (to be published).
- <sup>24</sup>E. K. Warburton, P. Gorodetzky, and J. A. Becker, to be published.
- <sup>25</sup>T. Engeland and P. J. Ellis, Nucl. Phys. **A181**, 368 (1972).
- <sup>26</sup>H. G. Benson and B. H. Flowers, Nucl. Phys. **A126**, 332 (1969).
- <sup>27</sup>A. P. Zuker, B. Buck, and J. B. McGrory, Phys. Rev. Lett. **21**, 39 (1968); A. P. Zuker, Phys. Rev. Lett. **23**, 983 (1969); J. B. McGrory, Phys. Lett. **31B**, 339 (1970); B. Buck, private communication.
- <sup>28</sup>S. J. Skorka, J. Hertel, and T. Retz-Schmidt, Nucl. Data **A2**, 347 (1966).
- <sup>29</sup>For a discussion of this point see E. K. Warburton and J. Weneser, in *Isospin in Nuclear Physics*, edited by D. H. Wilkinson (North-Holland, Amsterdam, 1969).

PHYSICAL REVIEW C

VOLUME 7, NUMBER 6

JUNE 1973

### Three-Neutron Pickup Reaction on <sup>13</sup>C†

E. Kashy, W. Benenson, I. D. Proctor, P. Hauge, and G. Bertsch

*Cyclotron Laboratory, Physics Department, Michigan State University, East Lansing, Michigan 48823*

(Received 5 February 1973)

Angular distributions of <sup>6</sup>He particles from the three-neutron pickup reaction <sup>13</sup>C(<sup>3</sup>He, <sup>6</sup>He)<sup>10</sup>C have been measured for transitions to the two lowest states of <sup>10</sup>C, the  $J^\pi = 0^+$  ground state and 3.35-MeV  $J^\pi = 2^+$  state. Observed anomalies in the shapes and magnitudes of these distributions cannot be explained theoretically by zero-range distorted-wave Born-approximation calculations.

#### I. INTRODUCTION

The (<sup>3</sup>He, <sup>6</sup>He) reaction has been used over the past three years principally for the precise measurement of masses of proton-rich nuclei in the 2s-1d shell.<sup>1</sup> These nuclei, such as <sup>25</sup>Si, are the  $T_z = -\frac{3}{2}$  member of isospin multiplets, and the resulting masses have provided a test of the isobaric multiplet mass equation. This reaction has also been recently used to extend our knowledge of proton-rich nuclei in the 1f<sub>7/2</sub> shell and also to obtain the spectra of these nuclei.<sup>2</sup> The extremely small cross sections which have been measured for the (<sup>3</sup>He, <sup>6</sup>He) reaction have inhibited the measurement of detailed angular distributions for most targets. A partial angular distribution for the <sup>12</sup>C(<sup>3</sup>He, <sup>6</sup>He)<sup>9</sup>C reaction measured earlier,<sup>3</sup> together with some angular distribution data on various targets, showed enough structure to make a strong case that a direct-reaction mechanism is principally involved in this reaction.

The present experiment is aimed at testing the reaction mechanism by studying a case in which both initial and final states are well known, the <sup>13</sup>C(<sup>3</sup>He, <sup>6</sup>He)<sup>10</sup>C reaction. The initial interest was inspired by a measurement of <sup>6</sup>He spectra at  $\theta_{\text{lab}}$

= 9° in which the yield to the  $J^\pi = 2^+$ , 3.35-MeV level of <sup>10</sup>C was found to be about 40 times greater than the yield to the  $J^\pi = 0^+$  ground state. This ratio aroused theoretical curiosity and also led to the present measurement of a more complete angular distribution for this reaction.

#### II. EXPERIMENTAL METHOD AND RESULTS

The <sup>13</sup>C(<sup>3</sup>He, <sup>6</sup>He)<sup>10</sup>C reaction was induced with 70.3-MeV <sup>3</sup>He from the Michigan State University cyclotron. The reaction particles were detected in an Enge split-pole spectrograph. The position on the focal plane was measured in a detection system consisting of a single-wire proportional counter with  $\frac{1}{2}$ -mil Kapton entrance and exit windows.<sup>4</sup> A thin plastic scintillator mounted on a photomultiplier tube was placed behind the proportional counter and provided time-of-flight information and also some particle discrimination based on the energy loss in the plastic scintillator.

A block diagram of the electronics used in the experiment is shown in Fig. 1. The setting of the various coincidence requirements is considerably simplified by the use of partial coincidence requirements. Thus the spectrum corresponding to

the time of flight of the reaction particles from the target to the plastic scintillator becomes easily recognizable when it is gated by coincident events from the proportional counter, since the procedure eliminates most of the  $\gamma$ -ray pulses in the plastic. The setting of the time window to select the rare  ${}^6\text{He}$  particles is facilitated by the presence of the far more numerous tritons, which for the same magnetic rigidity have the same time of flight. For particles other than  ${}^6\text{He}$ , precalculations of the flight-time spectrum of various reaction particles makes it possible to set the window accurately, and in addition reduces the confusion which results when the time of flight is greater than a single cyclotron period. Small changes in the time window were made during the taking of the angular-distribution data to take account of the rather large kinematic effects and hence magnetic-field changes required. This system in the focal plane of the spectrograph provides a high degree of particle discrimination and in addition is virtually 100% efficient.

The target consisted of a 0.2-mg/cm<sup>2</sup>-areal-density self-supporting foil of carbon enriched to 96% in  ${}^{13}\text{C}$ . A beam current of 0.4  $\mu\text{A}$  was used and the solid angle was defined by  $2^\circ \times 2^\circ$  slit (1.2 msr). Two of the  ${}^6\text{He}$  spectra measured are shown in Fig. 2, one for  $\theta_{\text{lab}} = 12^\circ$  and the second for  $\theta_{\text{lab}} = 24^\circ$ . It is apparent from these spectra that at  $12^\circ$  there is indeed a very small excitation of the  $J^\pi = 0^+$  ground state of  ${}^{10}\text{C}$ . It is worth noting that in spite of the very small cross sections the spectra include practically no background,

although a few counts between the peaks are present which may be due to the ( ${}^3\text{He}$ ,  ${}^6\text{He}$ ) reaction on slight contaminations of heavier atoms in the target.

The experimental results for the angular distributions are shown in Fig. 3. Both the  $J^\pi = 0^+$  ground-state and  $J^\pi = 2^+$  first-excited-state angular distributions show the rather marked structure which characterizes a direct reaction (or perhaps a direct surface reaction) process. It is indeed puzzling to see the degree of dissimilarity in the two angular distributions, especially since one would expect, in a simple picture, to see the same  $L$  transfer for both transitions. Before we discuss the theory and attempt to explain these unusual data, we note that the peak differential cross section of 3.5  $\mu\text{b}/\text{sr}$  in the angular distribution for the transition to the  $J^\pi = 2^+$   ${}^{10}\text{C}$  state represents the largest cross section we have measured for the ( ${}^3\text{He}$ ,  ${}^6\text{He}$ ) reaction in our investigations of this reaction on targets from carbon to lead.

### III. THEORY

In an effort to understand the mechanisms of the present reaction, standard distorted-wave Born-approximation (DWBA) calculations were made assuming a direct one-step process and using the zero-range approximation. The procedure for computing cross sections under these assumptions is well described in review articles,<sup>5</sup> so only a brief description is given below. However, the method used here for computing the radial over-

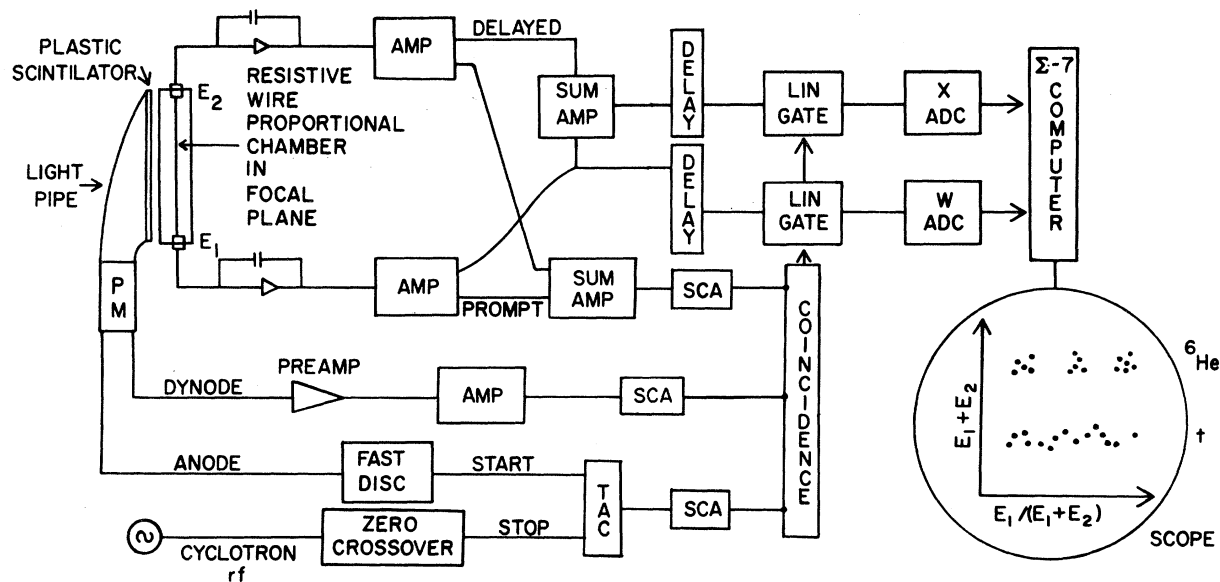


FIG. 1. Block diagram of the electronics used in the detection and identification of the  ${}^6\text{He}$  particles in the focal plane of the magnetic spectrograph.

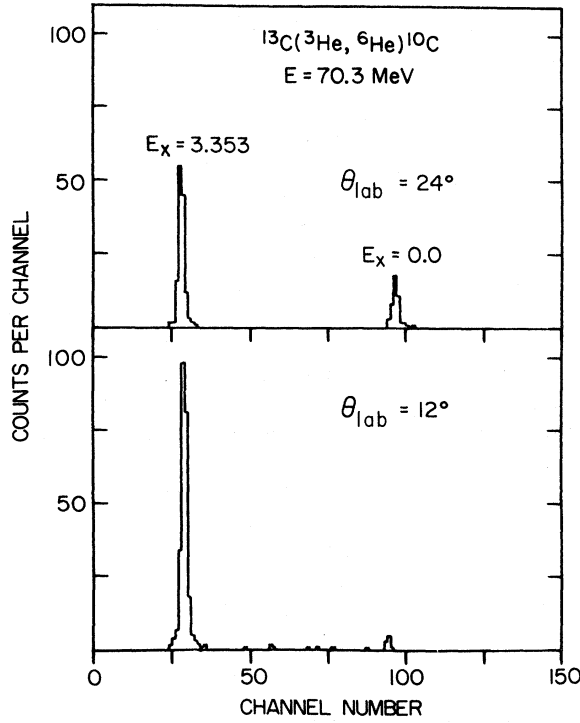


FIG. 2. Spectra of  ${}^6\text{He}$  particles at  $\theta_{\text{lab}} = 12^\circ$  and  $24^\circ$ . The integrated charge in each case was  $1000 \mu\text{C}$ . One channel corresponds to 50 keV in excitation.

laps in the three-nucleon-transfer form factor is different from that commonly used, and is therefore described in some detail.

If we denote the present reaction by  $A(a, b)B$ , the transition amplitude can be written as

$$T_{AB} \sim \int d\vec{r}_b d\vec{r}_a \psi^-(\vec{k}_b, \vec{r}_b) \psi^+(\vec{k}_a, \vec{r}_a) \times \left[ \int d\eta \psi_{m_b}^{s_b}(\vec{r}_b, \xi_b) V F_{M_B M_A}^{J_B J_A}(\vec{r}_1, \vec{r}_2, \vec{r}_3) \psi_{m_a}^{s_a}(\vec{r}_a, \xi_a) \right], \quad (1)$$

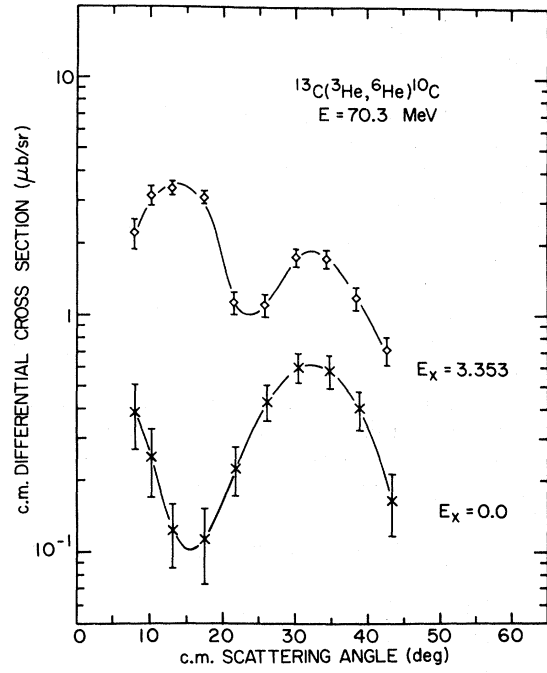


FIG. 3. Angular distributions of  ${}^6\text{He}$  particles for the  $^{13}\text{C}({}^3\text{He}, {}^6\text{He})^{10}\text{C}$  reaction to the  $0^+$  and  $2^+$  states of  $^{10}\text{C}$ . The solid lines are drawn through the experimental data.

where  $\psi^-$  and  $\psi^+$  are the scattering waves of the outgoing  ${}^6\text{He}$  and incoming  ${}^3\text{He}$  nuclei, respectively, and  $\psi_{m_b}^{s_b}(\vec{r}_b, \xi_b)$  and  $\psi_{m_a}^{s_a}(\vec{r}_a, \xi_a)$  are their corresponding internal wave functions. The quantity  $F_{M_B M_A}^{J_B J_A}(\vec{r}_1, \vec{r}_2, \vec{r}_3)$  is the nuclear overlap of the target and residual nucleus,  $V$  is the interaction potential between the incoming projectile and the three transferred neutrons, and  $\eta$  represents all nucleon coordinates other than the center-of-mass positions of  ${}^3\text{He}$  and  ${}^6\text{He}$  (i.e.,  $\vec{r}_a$  and  $\vec{r}_b$ ). The nuclear overlap is given in terms of the three-nu-

TABLE I. Quantities needed for computing transition strengths to the  $J^\pi = 0^+$  and  $2^+$  states in  $^{10}\text{C}$ .

Final state in $^{10}\text{C}$ $J^\pi T$	Quantum numbers of transferred neutrons			Transfer orbital momentum $L$	Overlap integral $g_{NL}^{JT}(\vec{r})$	Spectroscopic amplitudes		
	$J$	$T$	$N$			$JJ$ limit	Cohen and Kurath	Hauge and Maripuu
$0^+ 1$	$\frac{1}{2}$	$\frac{3}{2}$	2	1	$g(\vec{r})$	$-\sqrt{2}$	-1.187	-1.209
$2^+ 1$	$\frac{3}{2}$	$\frac{3}{2}$	3	1	$g(\vec{r})$	0	+0.807	+0.958
	$\frac{3}{2}$	$\frac{3}{2}$	1	1	$g(\vec{r})$	0	+0.277	+0.084
	$\frac{3}{2}$	$\frac{3}{2}$	2	1	0	$-\sqrt{4}$	-1.261	-1.488
	$\frac{5}{2}$	$\frac{3}{2}$	2	3	0	$+\sqrt{6}$	+1.520	+1.816

cleon spectroscopic amplitude  $S_N^{JT}$  by

$$F_{M_B M_A}^{J_B J_A}(\vec{r}_1, \vec{r}_2, \vec{r}_3) = \sum_{\substack{J T, N \\ M}} C(J_B J_A; M M_B M_A) S_N^{JT} \psi_{NM}^{JT}(\vec{r}_1, \vec{r}_2, \vec{r}_3), \quad (2)$$

where  $JT$  is the spin-isospin of the three transferred neutrons. The three-nucleon wave function  $\psi_N^{JT}$  is constructed from the  $jj$ -coupled shell-model functions as

$$\psi_{NM}^{JT}(\vec{r}_1, \vec{r}_2, \vec{r}_3) = \langle \vec{r}_1, \vec{r}_2, \vec{r}_3 | (p_{3/2})^N J T; (p_{1/2})^{3-N} J' T'; J T M \rangle, \quad (3)$$

where  $N$  is the number of nucleons in the  $p_{3/2}$  shell. Since all the three transferred particles are neutrons, we find that there are only five possible antisymmetric wave functions. These are uniquely specified by  $N$  and  $J$ , and are listed in Table I. Angular momentum conservation only allows  $J = \frac{1}{2}$  transfer to the  $J^\pi = 0^+$  ground state in  $^{10}\text{C}$ ; we see from the table that there is only one such function. The remaining four functions can contribute only to the  $J^\pi = 2^+$  excited state.

To evaluate the overlap integral inside the square brackets of Eq. (1), we first make the zero-range approximation,  $\vec{r}_a \approx \vec{r}_b$ . The overlap integral then factors into three separate terms, each containing three integrals over the coordinate space of a transferred particle. We also assume that the  $^6\text{He}$  wave function can be expressed in terms of the  $^3\text{He}$  wave function with the three extra neutrons in shell-model orbits about the  $^3\text{He}$ ,

$$\psi_{\delta\text{He}}(\vec{r}_b, \vec{\xi}_b) = \mathcal{G} \left\{ [(\psi)_{\delta\text{He}}^{1/2} \phi_{1s}(\vec{r}_b - \vec{r}_1)]^{L=0, S=0} \times [\phi_{1p}(\vec{r}_b - \vec{r}_2) \phi_{1p}(\vec{r}_b - \vec{r}_3)]^{L=0, S=0} \right\}. \quad (4)$$

In this expression  $\psi_{\delta\text{He}}^{1/2}$  is the  $^3\text{He}$  internal wave function,  $\phi_{ni}$  are single-particle wave functions,  $\mathcal{G}$  is the antisymmetrization operator, and the brackets denote spin and orbital angular momentum coupling. The angular dependence of the overlap integral can be made explicit by coupling the transferred nucleons to the  $^3\text{He}$  spins. We therefore redefine the overlap integral as

$$G_{NLM}^{JT}(\vec{r}) \equiv \left( \frac{4\pi}{2L+1} \right)^{1/2} g_{NL}^{JT}(\vec{r}) Y_{LM}(\hat{r}) = \int d\vec{\xi}_a d\vec{r}_1 d\vec{r}_2 d\vec{r}_3 \psi_0^0(\vec{\xi}_a, \vec{r} - \vec{r}_1, \vec{r} - \vec{r}_2, \vec{r} - \vec{r}_3) \times V[\psi_N^{JT}(\vec{r}_1, \vec{r}_2, \vec{r}_3) \psi^a(\vec{\xi}_a)]_M^L. \quad (5)$$

With the angular dependence specified by the coupling, we can determine the radial overlap,  $g_{NL}^{JT}(\vec{r})$ , by carrying out the nine integrations at only one angle. It was convenient to evaluate the integrals by rotating the projectile to the  $z$  axis, and using the  $m$  representation for the shell-model functions of Eqs. (3) and (4). We find, as expected, that only natural-parity transitions (i.e.,  $L=1$  or  $L=3$ ) are possible, as shown in Table I. Upon performing the three “ $z$ -coordinate” integrations with the  $LS$ -coupled  $^6\text{He}$  wave function of Eq. (4), we furthermore find that all radial overlaps have the same functional dependence on the projectile coordinate, and that the  $L=3$  overlap is identically zero. This is shown explicitly in column 4 of Table I. Under such circumstances, the calculated cross sections will have, unlike the data of Fig. 3, the same angular dependence, with a ratio depending only on the spectroscopic amplitudes (provided one neglects spin-orbit terms in the  $^3\text{He}$  and  $^6\text{He}$  optical potential). The theoretical ratio of the cross sections is found to be

$$R = \frac{\sigma(\theta)_{2^+}}{\sigma(\theta)_{0^+}} = \frac{1}{2} \left( \frac{S_1^{3/2, 3/2} + S_3^{3/2, 3/2}}{S_2^{1/2, 3/2}} \right)^2, \quad (6)$$

where the factor  $\frac{1}{2}$  comes from a statistical  $(2J+1)^{-1}$  dependence of the cross section on the square of the form factor. It arises when one sums over  $M_A$  and  $M_B$ , as can be seen from the Clebsch-Gordan coefficient in Eq. (2).

The spectroscopic amplitudes were computed for three representative sets of shell-model wave functions, using routines for one- and two-particle spectroscopic amplitudes in conjunction with the Oak Ridge shell-model code.<sup>6</sup> The resulting numbers are given in the last three columns of Table I. Note that the amplitudes from the “ $jj$ -coupling limit” are quite different from the other two more realistic calculations. The theoretical value<sup>7</sup> of  $R$  can be computed directly from Eq. (6) and Table I to be 0.417 and 0.371 for the shell-model states of Cohen and Kurath,<sup>8</sup> and Hauge and Maripuu,<sup>9</sup> respectively. From Fig. 3, we see immediately that there is a large discrepancy between experiment and theory. In fact, the experimental ratio of integrated cross section for angles up to  $\theta_{\text{c.m.}} = 45^\circ$  is  $R = 4.5$ , which is an order of magnitude larger than theory.

This variance can possibly be attributed to the approximations made in evaluating the integrals of Eq. (1). If higher-order corrections are included, we would expect only the  $J^\pi = 2^+$  cross section to change significantly; the  $J^\pi = 0^+$  cross section should retain its “zero-range” shape because it proceeds through only one channel (c.f. Table I). For this reason we compare only the data for the

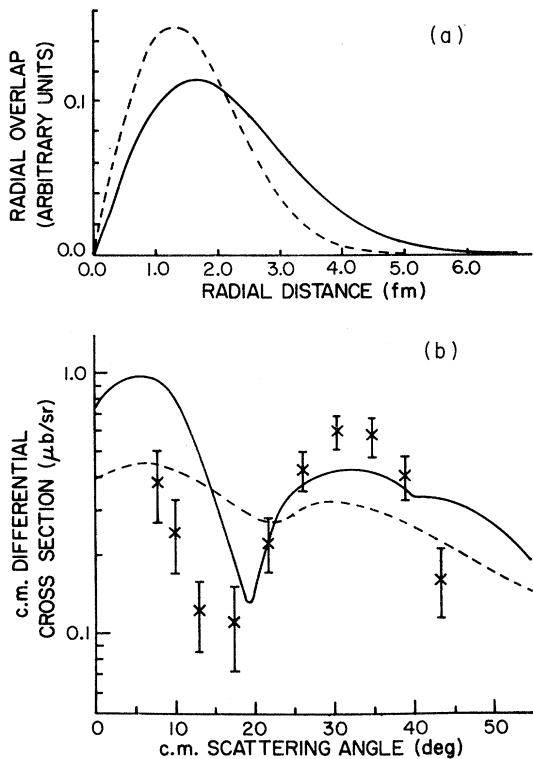


FIG. 4. (a), (b) The theoretical radial overlaps and cross sections are shown for the ground  $J^\pi = 0^+$  state in  $^{10}\text{C}$ . The solid and dashed curves correspond to using Woods-Saxon and harmonic-oscillator single-particle wave functions, respectively.

ground state of  $^{10}\text{C}$  with distorted-wave calculations. If the single-particle wave functions are assumed to be oscillator functions, the radial overlap of Eq. (5) can be determined analytically as

$$g(r) = Nr \exp\left[-\frac{3}{2} \frac{r^2}{(b_1^2 + b_2^2)}\right], \quad (7)$$

where  $N$  is a normalization constant, and  $b_1$  and  $b_2$  are the harmonic-oscillator size parameters for  $^6\text{He}$  and  $^{13}\text{C}$ , respectively. The dashed curve in Fig. 4(a) shows the radial overlap when we choose the size parameter to be 1.7 fm for both nuclei. We also evaluated the overlap using wave functions of a Woods-Saxon well with diffuseness  $a = 0.65$  fm, and radius  $R_0 = 1.5$  and 1.4 fm for  $^6\text{He}$  and  $^{10}\text{C}$ , respectively. (These parameters are similar to those of other works in the  $1p$  shell.<sup>10</sup>) The well depth  $V_0$  was then chosen so that the eigenenergies were consistent with the observed neutron separation energies in carbon and helium. The particular energies used were 0.50 MeV and 21.06 MeV for the  $1s$  and  $1p$  orbitals in  $^6\text{He}$ , and 12.37 MeV for the  $1p$  orbitals in  $^{13}\text{C}$ . The result-

ing radial overlap is shown by the solid curve in Fig. 4(a).

The cross sections in Fig. 4(b) were computed by numerically inserting the two radial overlaps into the zero-range DWBA code DWUCK of Kunz.<sup>11</sup> Rather than varying the optical-model  $^3\text{He}$  and  $^6\text{He}$  parameters to obtain agreement with experiment, these parameters were taken from previous experiments of  $^3\text{He}$  elastic scattering on  $^{27}\text{Al}$ ,<sup>12</sup> and ( $d, ^6\text{Li}$ ) reactions on several  $1p$  shell nuclei.<sup>13</sup> The parameters used, of course, have considerable uncertainty. However, reasonable variations of these parameters were considered and found to produce only minor changes in the cross-section shapes. As expected, the Woods-Saxon overlap yields results in much better agreement than does the oscillator approximation.

A final attempt to improve the theory was made by using the following more realistic  $^6\text{He}$  wave function<sup>8, 9, 14</sup>

$$\begin{aligned} \psi_{^6\text{He}} = & [\psi_{^3\text{He}}^{1/2} \phi_{1s}]^{S=0} \\ & \times \{0.95[\phi_{1p} \phi_{1p}]^{L=0, S=0} - 0.30[\phi_{1p} \phi_{1p}]^{L=1, S=1}\}. \end{aligned} \quad (8)$$

For this case, the radial overlaps are found to be nonzero for all five three-particle amplitudes, and consequently an  $L=3$  term does contribute to the  $J^\pi = 2^+$  cross section. A detailed calculation, however, shows that the corresponding changes in the cross section are quite small.

Thus these zero-range DWBA calculations explain, at most, only the yield to the ground state in  $^{10}\text{C}$ . From Eq. (6), we see that our failure to predict the relative magnitude of the  $J^\pi = 2^+$  cross section cannot be due to our lack of knowledge about the  $^3\text{He}$  and  $^6\text{He}$  optical potentials. Also, a careful analysis of the spectroscopic amplitude to the  $J^\pi = 0^+$  state reveals that this discrepancy is not caused by "accidental" cancellation of eigenvector components in  $^{10}\text{C}$  and  $^{13}\text{C}$ .

#### IV. CONCLUSIONS

The  $^{13}\text{C}(^3\text{He}, ^6\text{He})^{10}\text{C}$  reaction, in spite of its very weak cross section, appears to have angular distributions characteristic of direct surface reactions. However, the ratio of the yield to the ground and first excited states of  $^{10}\text{C}$  and the difference in the shapes of the angular distributions cannot be explained by simple DWBA zero-range theory even when reasonably realistic wave functions are used. It is probable that multiple step processes and other second-order effects are very important. The apparent selectivity of the

reaction is then probably not a nuclear structure effect, but rather a facet of the reaction mechanism. Future studies of the ( $^3\text{He}$ ,  $^6\text{He}$ ) reaction on targets of  $^{26}\text{Mg}$  and  $^{14}\text{C}$  will be useful in answering the questions posed by the present experiment.

## ACKNOWLEDGMENTS

The authors would like to thank Dr. B. H. WILDENTHAL for informative discussions concerning the computation of the one- and two-particle spectroscopic amplitudes.

<sup>1</sup>Supported by the National Science Foundation.

<sup>1</sup>G. F. Trentelman, B. M. Freedom, and E. Kashy, Phys. Rev. Lett. **25**, 530 (1970); R. Mendelson, G. J. Wozniak, A. D. Bacher, J. M. Loiseaux, and J. Cerny, Phys. Rev. Lett. **25**, 533 (1970); G. F. Trentelman and I. D. Proctor, Phys. Lett. B **35B**, 570 (1971).

<sup>2</sup>I. D. Proctor, W. Benenson, J. Driesbach, E. Kashy, G. F. Trentelman, and B. M. Freedom, Phys. Rev. Lett. **29**, 434 (1972).

<sup>3</sup>G. F. Trentelman, B. M. Freedom, and E. Kashy, Phys. Rev. C **3**, 2205 (1971).

<sup>4</sup>W. A. Lanford, W. Benenson, G. M. Crawley, E. Kashy, I. D. Proctor, and W. F. Steele, Bull. Am. Phys. Soc. **17**, 895 (1972).

<sup>5</sup>I. S. Towner and J. C. Hardy, Adv. Phys. **18**, 401 (1969); N. K. Glendenning, Annu. Rev. Nucl. Sci. **13**, 191 (1963).

<sup>6</sup>J. B. French, E. C. Halbert, J. B. McGrory, and S. S. M. Wong, in *Advances in Nuclear Physics*, edited by M. Baranger

and E. Vogt (Plenum Press, New York, 1969), Vol. 3, pp. 193-257.

<sup>7</sup>This ratio has also been calculated by D. Kurath, in an *LS*-coupling formalism, with similar results (private communication).

<sup>8</sup>S. Cohen and D. Kurath, Nucl. Phys. **73**, 1 (1965).

<sup>9</sup>P. S. Hauge and S. Maripuu, Phys. Rev. C (to be published).

<sup>10</sup>S. Kahana and D. Kurath, Phys. Rev. C **2**, 543 (1971); D. H. Wilkinson and M. E. Mafethe, Nucl. Phys. **85**, 97 (1966).

<sup>11</sup>P. D. Kunz, University of Colorado (unpublished).

<sup>12</sup>C. B. Fulmer and J. C. Hafele, Phys. Rev. C **5**, 1969 (1972).

<sup>13</sup>H. H. Gutbrod, H. Yoshida, and R. Bock in *Nuclear Reactions Induced by Heavy Ions*, edited by R. Bock and W. R. Hering (North-Holland and American Elsevier Publishing Companies, 1970) p. 311.

<sup>14</sup>F. C. Barker, Nucl. Phys. **83**, 418 (1966); J. L. Norton and P. Goldhammer, Nucl. Phys. **A165**, 33 (1971).

## Optical Potential for Scattering from a System of Finite-Mass Particles\*

G. E. Walker

Department of Physics, Indiana University, Bloomington, Indiana 47401

(Received 29 December 1972)

We consider a projectile scattering elastically from a system of finite-mass constituents via a separable microscopic interaction. In order to reduce the situation to a solvable problem, several standard assumptions are necessary. The validity of these assumptions can be checked in a given model problem. The optical potential is identified by comparing the multiple scattering series we obtain with that obtained in the equivalent one-body problem. The optical potential explicitly exhibits the effects of the Fermi motion and finite mass of the target particles and is a generalization of an optical potential obtained earlier. Our results are in a form suitable for application to intermediate energy projectile many-body target scattering.

## I. INTRODUCTION

The concept of the optical potential has been extremely useful for reducing the complexities of the many-body elastic scattering problem to the simplicity of the equivalent one-body problem. Optical potentials not only provide a convenient way of describing elastic scattering but yield valuable input, in the form of distorted waves, for currently fashionable approaches to inelastic scattering and reaction processes such as the distorted-wave Born approximation. Of course one wishes

to understand the relationship between the optical potential and the more elementary interactions between the (perhaps complex) projectile and the individual constituents of the target. In this way, for example, one may limit the geometrical forms adopted for the optical potential whose parameters are to be obtained by fitting to a given experiment. In addition, by studying microscopic theories of the optical potential one gains some insight into (1) the limits of validity of the concept and (2) the dependence of the optical potential on the energy of the projectile and the detailed characteristics